Available online at www.sciencedirect.com

SCIENCE DIRECT®

Earth and Planetary Science Letters 227 (2004) 185–199

EPSL

www.elsevier.com/locate/epsl

Global inventory of methane clathrate: sensitivity to changes in the deep ocean

Bruce Buffett*, David Archer[1]

Department of Geophysical Sciences, The University of Chicago, Chicago, IL 60637, USA

Received 14 April 2004; received in revised form 10 August 2004; accepted 1 September 2004
Available online 8 October 2004
Editor: E. Bard

Abstract

We present a mechanistic model for the distribution of methane clathrate in marine sediments, and use it to predict the sensitivity of the steady-state methane inventory to changes in the deep ocean. The methane inventory is determined by binning the seafloor area according to water depth, temperature, and O_2 concentration. Organic carbon rain to the seafloor is treated as a simple function of water depth, and carbon burial for each bin is estimated using a sediment diagenesis model called Muds [Glob. Biogeochem. Cycles 16 (2002)]. The predicted concentration of organic carbon is fed into a clathrate model [J. Geophys. Res. 108 (2003)] to calculate steady-state profiles of dissolved, frozen, and gaseous methane. We estimate the amount of methane in ocean sediments by multiplying the sediment column inventories by the corresponding binned seafloor areas. Our estimate of the methane inventory is sensitive to the efficiency of methane production from organic matter and to the rate of fluid flow within the sediment column. Preferred values for these parameters are taken from previous studies of both passive and active margins, yielding a global estimate of 3×10^{18} g of carbon (3000 Gton C) in clathrate and 2×10^{18} g (2000 Gton C) in methane bubbles. The predicted methane inventory decreases by 85% in response to 3 °C of warming. Conversely, the methane inventory increases by a factor of 2 if the O_2 concentration of the deep ocean decreases by 40 μM or carbon rain increases by 50% (due to an increase in primary production). Changes in sea level have a small effect. We use these sensitivities to assess the past and future state of the methane clathrate reservoir.

Keywords: gas hydrates; carbon cycle; global change; early diagenesis

1. Introduction

Large amounts of methane are sequestered in marine sediments by an icy solid called methane clathrate (or methane hydrate). Estimates of the global inventory of methane clathrate may exceed 10^{19} g of carbon [3–5], which is comparable to estimates of potentially

* Corresponding author. Tel.: +1 773 702 8107; fax: +1 773 702 9505.
E-mail addresses: buffett@geosci.uchicago.edu (B. Buffett), d-archer@uchicago.edu (D. Archer).
[1] Tel.: +1 773 702 0823; fax: +1 773 702 9505.

0012-821X/$ - see front matter © 2004 Elsevier B.V. All rights reserved.
doi:10.1016/j.epsl.2004.09.005

recoverable coal, oil, and natural gas [6]. The proximity of this methane reservoir to the seafloor has motivated speculations about a release of methane in response to climate change [7,8]. Increases in temperature or decreases in pressure (through changes in sea level) tend to dissociate clathrate, releasing methane into the near-surface environment. Release of methane from clathrate has been invoked to explain abrupt increases in the atmospheric concentration of methane during the last glacial cycle [9]. A more catastrophic release of methane from clathrate has been proposed [10] to explain an isotopic excursion and a mass extinction of benthic foraminifera at the end of the Paleocene [11,12]. Terrestrial and oceanic values of $\delta^{13}C$ decreased by 2–3‰ [13], consistent with a release of $1–2\times10^{18}$ g of methane carbon from clathrate [14,15]. A nearly simultaneous change in $\delta^{18}O$ in the deep ocean indicates a temperature increase of 4–6 °C. The initial excursions in $\delta^{18}O$ and $\delta^{13}C$ occurred in less than 10^4 years, whereas the recovery lasted 10^5 years [16], comparable to the time required for silicate weathering to restore the atmospheric concentration of carbon dioxide [17].

Two issues are important for assessing the role of methane clathrate in the carbon cycle. First, the clathrate reservoir must be large enough to influence the carbon cycle. This appears to be the case at present, but greater uncertainty exists during the Paleocene when warmer ocean temperatures reduce the region of clathrate stability [18]. Second, we need to know how the clathrate inventory responds to changes in the deep ocean. The time scale for this response is important because slow, diffusive loss of methane probably results in oxidation by sulfate and precipitation to $CaCO_3$ within the sediments [19], with negligible effect on climate. A faster response allows methane oxidation within the ocean, which increases the concentration of CO_2 in the atmosphere. Support for a rapid release of methane at the end of the Paleocene is inferred from the abrupt excursion in terrestrial and oceanic values of $\delta^{13}C$. Such rapid release can occur through slumping of continental slopes [20] or by pervasive flow along fractures due to overpressured gas below the seafloor [21]. These mechanisms may permit methane to enter the ocean or atmosphere directly. The onset of catastrophic methane release is probably dependent on the abundance and spatial distribution of clathrate and methane bubbles in the sediments prior to failure. Because the spatial distribution of methane also determines the global inventory, the size and response of the clathrate reservoir are interconnected.

Current estimates of the global inventory of methane clathrate have been inferred from empirical correlations, often based on observations at a few well-studied sites. Kvenvolden [3] estimated the amount of methane clathrate in marine sediments by determining the area of the ocean in which sediments accumulate with an organic content in excess of 1% (dry weight). The abundance of clathrate per square meter was based on the assumption that clathrate occupies 10% of the pore volume in the sediments and that the average thickness of the stability zone was 400 m. Combining these estimates yields an inventory of 2.1×10^{19} g of methane carbon (denoted g C). Different choices for the required organic content [4,22] or the volume fraction of clathrate [4,5,23] yield substantially different estimates for the inventory. Uncertainties inevitably arise when observations from a few locations are extrapolated over the entire ocean (see [24] for a review). For example, variations in oxygen concentration in the deep ocean can strongly affect the preservation of carbon in sediment. The resulting volume fraction of clathrate can vary with sedimentation rate, seafloor temperature, and the efficiency of microbial conversion of organic carbon to methane [25]. Our approach to this problem is to use available observations to constrain the mechanisms responsible for clathrate formation. A quantitative model (described in Section 3) is then be used as the basis for extrapolation.

2. Areal extent and local abundance of methane clathrate

Methane clathrate is confined to the top few hundred meters of marine sediment. The zone of stability is specified using the phase diagram for methane and water (see Fig. 1). Clathrate is stable when the temperature is at or below the value $T_3(P)$ for three-phase equilibrium between clathrate, liquid water, and methane gas. Experimental determinations of $T_3(P)$ are shown in Fig. 1 as a function of depth, assuming a hydrostatic increase in pressure. Superimposed on this figure is a schematic illustration of the temperature

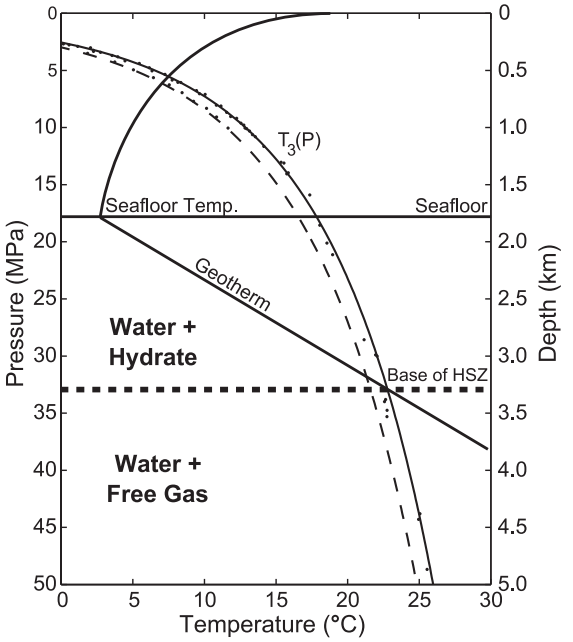

Fig. 1. Schematic illustration of temperature through the ocean and uppermost marine sediments. The temperature for clathrate stability, T_3(P), increases with pressure (or depth). Experimental data for T_3(P) in pure water (dashed line) and seawater (solid line) are extrapolated using a thermodynamic model [50]. The base of the stability zone is defined by the intersection of the geotherm with T_3(P).

profile through the ocean and sediments. The zone of stability is limited by the intersection of the local temperature profile with T_3(P), although clathrate is confined to the sediments because the concentration of methane in the ocean is too low to form clathrate, and the buoyancy of clathrate in seawater would carry it out of the stability zone, even if it did form.

Clathrate is unlikely to form below water depths of less than 600 m because the bottom water is too warm for stability. One exception occurs in the Arctic Ocean where water temperatures as low as -1.5 °C permit clathrate to form at depths of only 250 m. Elsewhere, clathrate is commonly found below intermediate water depths of 1000 to 3000 m [26]. As the depth of the water increases, and the temperature of the seafloor decreases, the zone of stability becomes thicker and capable of accommodating larger volumes of clathrate. However, clathrate has never been detected in sediments in the abyss, presumably because the rate of carbon rain to the seafloor is too low to supply the required source of methane through microbial conversion of organic material in the sediments [27]. In fact, 90% of the global carbon burial is thought to occur at water depths of less than 1000 m [1], where the depth of clathrate stability is comparatively thin. This interplay between the depth of the stability zone and the rate of carbon rain to the seafloor appears to limit clathrate to intermediate water depths.

Estimates of clathrate abundance often distinguish between passive and active margins [5]. The abundance of clathrate on passive margins is thought to be low (typically 5% to 10% of the pore volume [28]) because the supply of methane is limited by the availability of organic material in the sediments. On the other hand, active margins are thought to have much higher clathrate volumes, perhaps occupying as much as 30% to 50% of the pore space [5,29,30]. Such large volumes are attributed to pervasive fluid flow that scavenges methane from a broader region [31]. While estimates of fluid flow at active margins often exceed several mm year^{-1} [32], the evidence for widespread accumulation of large clathrate concentrations is equivocal. Modeling studies [33] show that volume fractions of 30% to 50% on the Cascadia margin, offshore Vancouver Island, are incompatible with pore-water chloride concentrations from ODP Site 146. More recent in situ measurements of methane concentration from Hydrate Ridge, offshore Oregon, suggest that high volume fractions of clathrate are confined to localized faults, and that broader regions are characterized by volume fractions of a few percent [23].

In this study, we assume that the primary source of methane is from conversion of organic carbon in the sediments. The input of carbon at the seafloor is converted to methane once the organic material is buried below the sulfate-reducing zone. Methane is transported through the sediments by diffusion and by pore-fluid flow. Fluid flow recycles and traps methane more efficiently within the clathrate zone, yielding higher clathrate volumes in high-flow active margins. The model-predicted global inventory of clathrate is particularly sensitive to the efficiency of methane production from organic matter and to the rate of fluid flow. However, the response of the model to changes in climatic and geochemical forcing is perhaps more robust, especially if the fluid flow and efficiency of methane production are insensitive to climate.

3. Description of the model

The inventory of methane clathrate below the seafloor is ultimately controlled by the supply of carbon. We quantify the flux of carbon to the seafloor using a parameterization of the ocean carbon cycle and predict the efficiency of carbon burial using a sediment diagenesis model. Once the organic material is buried below the sulfate-reducing zone, methanogens convert a fraction of this carbon to methane. The resulting distribution of methane in dissolved, gaseous, and clathrate phases is predicted using a clathrate model. Each component of the model is briefly described below.

3.1. Carbon rain

Organic carbon rain to the seafloor is strongly correlated with water depth (see Fig. 2a). This reflects the fact that shallow waters are typically close to coastlines, where particulate organic carbon production and recycling are rapid. Primary production rates in coastal waters are elevated severalfold over open-ocean rates by coastal upwelling, nutrient runoff from rivers, and nutrient recycling from the shallow sediments. Sediments in coastal waters participate in nutrient recycling because they are closer to the euphotic zone, whereas nutrient recycling in deeper water does not reach the seafloor. As a result, the benthic flux of organic matter is amplified in near-shore regions even more intensely than primary production is amplified. With the increase in organic carbon and terriginous material (clay) rain, the burial efficiency of shallow-water sediments increases as well, to up to ~50% preservation (compared to just a few percent in pelagic sediments). These factors conspire to greatly amplify the burial of organic matter in near-shore sediments, so that shallow waters account for ~90% of organic carbon burial in the global ocean.

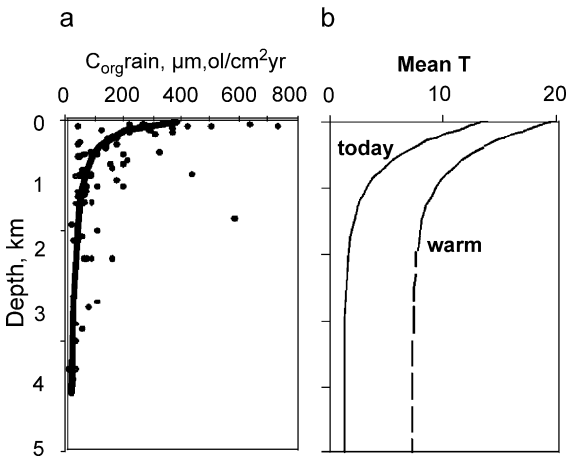

Fig. 2. (a) A summary of measurements of organic carbon rain to the seafloor as a function of water depth. The solid line represents the best-fitting curve through the data, while the scatter indicates the regional variability. (b) Average temperature profile in the ocean as a function of depth for present-day and warmer conditions.

Our approach is to treat organic rain as a simple function of water depth. The depth dependence is determined by fitting a curve through the data shown in Fig. 2a. This approach is commonly used to parameterize carbon rains in models of the ocean carbon cycle [1,34]. The weakness of the approach is that it does not account for lateral heterogeneity in primary production or shelf/slope dynamics. These influences are reflected in the scatter of the data. The best-fit curve represents a spatial average of the carbon rain, which is suitable for estimating global inventories. However, we are unable to predict regional anomalies in the geographic distribution of methane clathrate without resorting to a spatially dependent description of the carbon rain. Such extensions are possible and could be applied without altering the other components of our model.

3.2. Early diagenesis model

Most of the organic carbon rain to the seafloor is respired rather than buried, and the fraction buried below 1 m depth is determined by the oxidation/reduction chemistry of the sediment and the kinetics of biogenic reactions, such as respiration, bioturbation, and sediment irrigation. We employ a sediment diagenesis model called Muds, which solves for organic degradation reactions within the top meter of the sediment [1]. Muds is based on steady state diffusion-reaction equations for pore water and solid sediment. The model equations and reaction kinetics are similar to previously published sedimentary diagenetic models [35,36], but steady-state solutions are obtained directly using an efficient relaxation method.

Rate constant parameterizations in Muds were tuned using a simulated annealing method to reproduce solid-phase organic carbon and MnO_2, and pore-water NO_3^-, NH_4^+, Mn^{2+}, Fe^{2+}, and H_2S data [1]. Rate constants for respiration, bioturbation, and pore-water irrigation by benthic macrofauna are parameterized in terms of the total organic carbon rain rate and overlying water O_2. The organic carbon initially reacts with O_2 in the pore water, then passes through the NO_3^-/MnO_2 and $SO_4^-/FeOOH$ redox zones. Oxic respiration rate constants are significantly higher than anoxic rates, so that organic carbon preservation is sensitive to the O_2 concentration as well as the organic carbon rain. The model is fairly successful at predicting the organic carbon concentration in the sediments, with no "site-custom tuning", based only on rain rates and the O_2 concentration in the overlying water. The model formulation, parameterizations, and tuning, were all used as presented in [1], with no adjustment or revision. The relevant output of the model includes the organic carbon concentration and the total sediment accumulation rate.

3.3. Clathrate model

We adopt a steady-state model [2] to describe the distribution clathrate in the top few hundred meters of sediment. The steady-state distribution develops after ~10^6 years of accumulations [25], and reflects the average environmental conditions over this time interval. It is also possible to use time-dependent models, in principle, although we currently lack detailed knowledge of the relevant history to implement such a model. The depth of the stability zone in all calculations is determined from the phase diagram using the seafloor temperature, geothermal gradient, water depth and salinity. (We adopt a constant salinity of 0.035 and assume a constant geothermal gradient of 0.04 K/m on passive margins and 0.06 K/m on active margins.) The model also includes a region of several hundred meters below the base of the stability zone to describe the accumulation of gas bubbles and a sulfate-reducing zone in the top 10–20 m, depending on the upward flux of methane toward the seafloor (see [2] for details).

The primary source of methane in the model is from conversion of organic carbon in the sediments. Our emphasis on biological sources of methane is motivated by the light isotopic composition of carbon recovered from samples of clathrate (typically $\delta^{13}C = -60‰$), which suggests that thermogenic sources of methane are not important in most cases [37]. We include the possibility of a deep source of methane by permitting methane-bearing fluid to migrate from below. The significance of this deep source depends on the methane content of the incoming fluid. We consider fluids with a methane concentration of 50% the saturation level, which is low enough to prevent clathrate from accumulating without converting organic material to methane inside the model domain. The incoming fluid often becomes saturated with methane as it rises through the region of gas bubbles below the clathrate stability zone, so the primary role of fluid flow is to recycle methane from bubbles back into the stability zone.

Conversion of organic carbon to methane occurs once the organic material is buried below the sulfate-reducing zone. The rates of sedimentation and carbon burial from Muds are used as input parameters in the clathrate model. Other input parameters in the clathrate model include the fraction of buried carbon available to methanogens and the associated rate constant for carbon consumption. Values for these parameters are taken from previous studies [33,38], which fit model predictions to pore-water sulfate and chloride concentrations from ODP Leg 164 (Blake Ridge). The same parameter values also yield a good fit to pore-water sulfate and chloride concentrations from ODP Leg 146 (Cascadia Margin). The clathrate model routinely accounts for sediment compaction and fluid expulsion, assuming an exponential decrease in sediment porosity with depth [39]. An additional flow is superimposed on the fluid expulsion to account for deeper sources of fluid. In this study, we assume that the deeper source of fluid is driven by pressure that develops under nonsteady or nonuniform compaction of the sediments [40]. We express the net fluid flow as an interstitial velocity at the seafloor and relate the amplitude of the velocity to the sedimentation rate. This fluid velocity is intended to represent a regional average, which we apply in an upward direction over 50% of the area and downward over the remaining area. A range of values are explored in this study, but we ultimately adopt the fluid velocities inferred from comparisons of the model predictions with pore-water analysis from ODP Legs 146 and

164. (Details of the model assumptions and fitting procedure are given in [33,38].)

4. Global inventory of methane clathrate

The procedure for calculating the present-day inventory of methane clathrate can be summarized as follows. The area of the seafloor is tabulated into bins of water depth and O_2 concentration using the ETOPO5 5-min bathymetry and Levitus et al. [41] distribution of O_2. The depth bins coincide with the 33 levels from Levitus et al. [41], and the O_2 concentration is binned in increments of 10 μM. We find nearly equivalent results treating temperature in each of two ways. In one calculation, the seafloor temperature is treated as a simple function of depth, based on the average (present-day) temperature profile in the ocean (Fig. 2b). In a second calculation, we bin the seafloor area according to water temperature, in addition to water depth and O_2, beginning at −1 °C and increasing in increments of 2 °C.

The diagenesis model is run for the conditions of each sediment area bin, and the results are fed into the clathrate model, to estimate mass of methane in clathrate and gas bubbles per square meter. The global inventory of clathrate is tallied by multiplying the result by the area of sediment which exists under the conditions of each bin.

A typical result of the calculation is shown in Fig. 3. High concentrations of organic carbon accumulate when the water depth is shallow or the O_2 concentration near the seafloor is low. Clathrate is not stable in shallow water, so most of the clathrate occurs at low O_2 concentrations. Multiplying the abundance of clathrate by the seafloor area yields the global

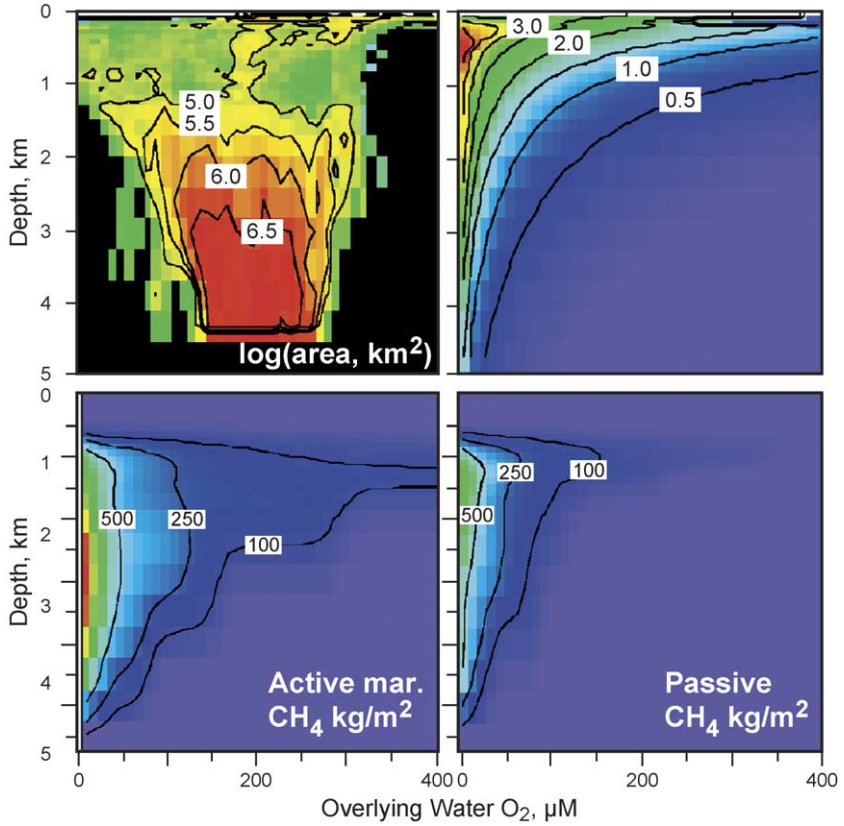

Fig. 3. Representative estimates for (a) the seafloor area in km^2, (b) the concentration of organic carbon in percent dry weight, and (c) the abundance of clathrate methane in kg/m^2. We include two calculations for the clathrate abundance using conditions appropriate for a passive and active margin.

inventory. We give two examples for the clathrate abundance using estimates of fluid flow appropriate for passive and active margins. The higher fluid flow at active margins increases the abundance of clathrate inventory by recycling methane back into the stability zone. As a result, clathrate is found over a broader range of O_2 concentration and depth in the active margin case.

The sensitivity of the global inventory to fluid flow is shown in Fig. 4. The fluid velocity refers to the upward interstitial velocity at the seafloor, expressed as a fraction of the sedimentation rate. The composition of the fluid entering the base of the model domain is specified in terms of the local methane saturation [38]. We assume that the incoming fluid is 50% saturated with methane, although the predictions are not sensitive to this choice. The lack of sensitivity to a deep methane source indicates that most of the methane is derived from organic material within the model domain. We also consider a range of values for the efficiency of methane production from organic matter. A carbon conversion of 50% probably represents an upper limit, so the results obtained with this conversion give an upper bound on the methane inventory. A more plausible conversion of 25% is used in the calculations shown in Fig. 3. Adopting

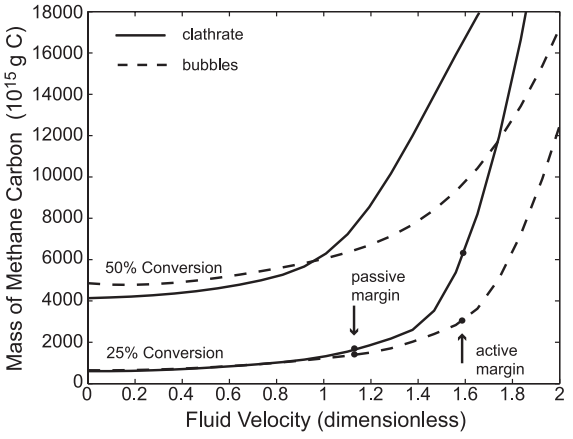

Fig. 4. The inventory of methane in clathrate and gas bubbles as a function of fluid flow through the sediments. The efficiency ψ of methane production from organic matter is fixed at 25% and 50%. The fluid velocity v_f refers to the upward interstitial velocity at the seafloor. The magnitude of v_f is expressed in terms of the sediment velocity v_s (e.g., sedimentation rate). The passive margin case is defined by v_f=1.18 v_s and the active margin case is defined by v_f=1.6 v_s.

lower values for the carbon conversion has a dramatic effect on the clathrate inventory. For example, the clathrate inventory with no imposed flow drops from 4.2×10^{18} to 0.6×10^{18} g C when the carbon conversion is reduced from 50% to 25%. Reducing the carbon conversion to 10% (not shown in Fig. 4) decreases the clathrate inventory to a meager 4.4×10^{15} g C.

The choice of parameter values is based on the results of previous modeling studies at sites from ODP Leg 146 on the Cascadia margin and ODP Leg 164 on the Blake Ridge [2,33]. Many of the model inputs, including the sedimentation rate, carbon burial, seafloor temperature, and geothermal gradient are inferred from the drill core or well logging [42,43]. The remaining model parameters, notably the fraction of carbon available to methanogens and the fluid velocity, were estimated by fitting the model predictions to observations of pore-water chloride and sulfate concentration. On the Blake Ridge, the best fit to the observations was obtained using 25% carbon conversion and a fluid flow of 0.23 mm year^{-1} [2], which is slightly greater than the average sedimentation rate v_s. The choice of 25% carbon conversion on the Cascadia margin also provides a good fit to the observations when the fluid flow is 0.4 mm year^{-1}, or about 1.6 times greater than v_s. Applying the parameters for Blake Ridge (a passive margin) to all continental margins yields a global inventory of 1.8×10^{18} g C in clathrate and 1.4×10^{18} g C in gas bubbles. A larger inventory of 6.7×10^{18} g C in clathrate and 2.8×10^{18}g C in bubbles is obtained using the parameters appropriate for Cascadia (an active margin). Our best estimate is obtained by weighting these inventories by the fractional area of passive and active margins. Assuming 75% passive margin and 25% active margin, we obtain 3.0×10^{18} g C in clathrate and 1.8×10^{18} g C in bubbles for a total of 4.8×10^{18} g (4800 Gton C). The partitioning of carbon between clathrate and bubbles is compatible with recent observational estimates [44].

Fluid flow alters the clathrate inventory primarily by changing the area where clathrate occurs. Clathrate is predicted in sediments with as little as 0.5% (dry weight) organic carbon when the fluid flow is 1.6 v_s. The area of the seafloor with sediments containing more than 0.5% organic carbon is 2.3×10^7 km^2 in the present-day ocean. A higher concentration of organic

carbon (~1% dry weight) is required when the fluid velocity is reduced to 1.18 v_s. The corresponding area of the seafloor reduces to 0.98×10^7 km^2 (or 2.7% of the seafloor area), which is very close to the value assumed in the global inventory of Kvenvolden [3]. The change in seafloor area accounts for most of the change in clathrate inventory when the fluid flow is varied from passive to active margin conditions. The remainder of the change in inventory is due to a modest change in the volume fraction of clathrate and bubbles in the sediment. Fig. 5 shows a series of predictions for the distribution of clathrate below the seafloor using both passive and active margin conditions. In these representative calculations, the volume of clathrate increases with depth below the seafloor, reaching a peak value at the base of the stability zone. The highest value using passive-margin conditions is about 4%, whereas the active margin conditions yield a peak value of 6%. A slightly larger volume fraction is predicted when the O_2 concentration is decreased from the representative value used in Fig. 5, but even the highest concentration of clathrate rarely exceeds 10% of the pore volume, and the depth average at any site is typically much less than 10%. In fact, the average concentration over the entire reservoir is approximately 2%. Not surprisingly, our estimate of the clathrate inventory is much lower than that of Kvenvolden [3], which was based on the assumption of a 10% volume fraction.

Substantially lower clathrate inventories (500–2500 Gton C) have recently been proposed [23,24] on the basis of new observations collected from ODP Leg 204 (Hydrate Ridge). The volume of clathrate off the main ridge is thought to be less than a few percent of the pore volume [23], which is lower than previous estimates from ODP Legs 146 and 164. When the clathrate model is applied to Site 1245 of Leg 204 using the carbon conversion and fluid flow adopted in this study, we obtain a clathrate volume of approximately 1% in the lowermost 50 m of the stability zone (see Appendix A). The low clathrate volume is due mainly to the shallow water depth (870 m at Site 1245), which is not characteristic of most clathrate locations. As a result, global extrapolations based on the results of Leg 204 may underestimate the clathrate inventory. On the other hand, model predictions obtained with a common set of parameter values are compatible with results from ODP Legs 146, 164, and 204, illustrating the utility of extrapolating physical processes rather than clathrate volumes directly.

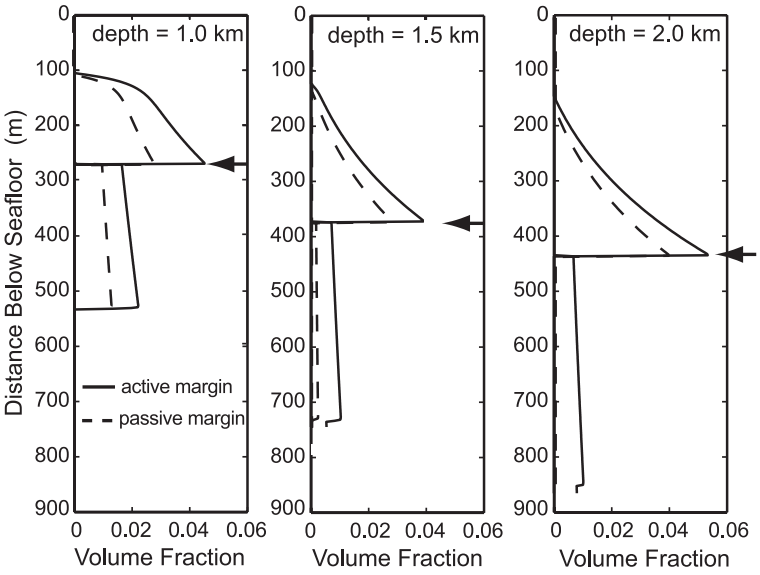

Fig. 5. Vertical distribution of clathrate and bubble volume below the seafloor for several choices of water depth. The O_2 concentration near the seafloor is fixed at 45 μM in each calculation. The distinction between passive and active margin conditions is based on the interstitial fluid flow at the seafloor. The passive margin case is defined by v_f=1.18 v_s and the active margin case is defined by v_f=1.6 v_s, where v_s is the sedimentation rate.

5. Sensitivity to changes in the deep ocean

Doubling the present-day concentration of carbon dioxide is expected to increase the average atmospheric temperature by roughly 3 °C [45,46]. As higher temperatures propagate into the deep ocean and seafloor, the inventory of clathrate is expected to decrease. We can quantify the change by repeating our calculations using a warmer seafloor temperature. The effect of changes in other conditions, including sea level, O_2 concentration, and carbon rain, can be assessed in a similar way. Unfortunately, the change in a steady-state solution does not reveal how this transition occurs. The transition could be extremely gradual, paced by the time scales of sediment accumulation and methane loss by diffusion. Or it could be catastrophic, triggered by submarine landslides and amplified by a positive feedback due to increases in greenhouse gases. As first step toward distinguishing between these possibilities, we establish the sensitivity of the inventory to changes in the deep ocean with the understanding that transitions could last ~10^6 years. In this section, we examine the effect of changes in temperature, O_2 concentration, sea level, and carbon rain using our preferred present-day estimate as a starting point.

5.1. Changes in temperature

An increase in temperature lowers the clathrate inventory by changing the depth of clathrate stability in the sediments. Part of the decrease in inventory is due to a reduction in sediment volume where clathrate is stable [18]. A second, more important, contribution arises from increases in the diffusive loss of methane toward the seafloor. The burial of organic carbon must increase to compensate for the increased losses, reducing the area of the seafloor where clathrate can form. This combination of factors produces a rapid drop in the methane inventory as temperature increases at the seafloor. The results shown in Fig. 6 are obtained by allowing the depth-dependent temperature in Fig. 2 to shift to the warm conditions. The temperature change is referenced to a depth of 1 km. For a plausible temperature increase of 3 °C, the inventory of methane in clathrate and bubbles decreases to 7.2×10^{17} g C, or about 15% of the present inventory.

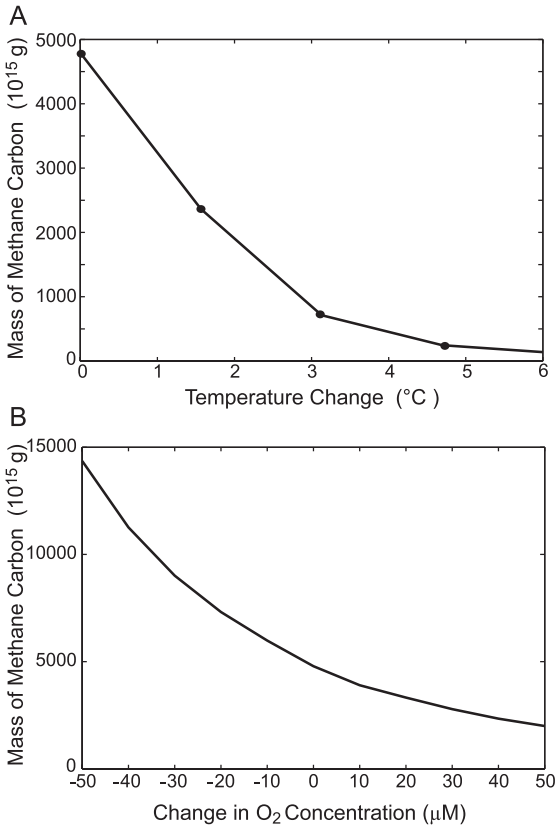

Fig. 6. Change in steady-state methane inventory in response to changes in (A) seafloor temperature and (B) O_2 concentration near the seafloor. The change in inventory is defined relative to our best estimate for the present day.

The strong temperature dependence of the clathrate inventory can be understood and quantified by considering a simple mass balance for methane inside the clathrate stability zone. Diffusive loss of methane at the seafloor can be approximated by

$$F = Dc(d)/d \tag{1}$$

where $c(d)$ is the concentration of methane at the base of the stability zone, d is the depth of the stability zone and D is the diffusion coefficient for methane in seawater. This rate of methane loss is balanced by a methane source to maintain a steady state. The net methane source is

$$\Phi = \int_0^d \phi dz \sim \phi d \tag{2}$$

where ϕ is the rate of conversion of organic carbon to methane (per unit volume). In the clathrate model, we

express ϕ as a linear function of the organic carbon concentration α in the sediments and assume that only a fraction ψ of α is converted to methane. In this approximation, the methane source becomes

$$\Phi \sim k\psi\alpha d \tag{3}$$

where the rate constant k includes the conversion between the units of α (% dry weight) and c (mass fraction of the pore liquid). Equating the source Φ and the loss F yields

$$\alpha = Dc(d)/k\psi d^2 \tag{4}$$

which relates the organic carbon in the sediments to the concentration of dissolved methane at the base of the stability zone. Clathrate becomes stable when $c(d)$ equals the local solubility $c_{eq}(d)$, so the minimum value of α is given by

$$\alpha_{min} = Dc_{eq}(d)/k\psi d^2 \tag{5}$$

As the depth of the stability field decreases, the concentration of organic carbon in sediments must increase in order satisfy Eq. (5). [The depth dependence of $c_{eq}(d)$ is fairly weak due to the counteracting effects of pressure and temperature]. The area of the seafloor with organic carbon in excess of α_{min} can be approximated by

$$A(\alpha_{min}) \sim A(\alpha_0)(\alpha_0/\alpha_{min})^{3/2} \tag{6}$$

where $A(\alpha_0)$ is the area of the seafloor with organic carbon in excess of α_0=1% (roughly the area of the present-day inventory). The corresponding volume of the present-day inventory is defined by $V(d_0)$=$A(\alpha_0)$ d_0, where d_0 is the average depth of the stability zone. When the average depth d decreases due to warming, the value of α_{min} goes up, according to Eq. (5), and the area $A(\alpha_{min})$ goes down, according to Eq. (6). The volume of the clathrate inventory can be estimated by combining Eqs. (5) and (6) to yield

$$V(d)/V(d_0) \sim (d/d_0)^4 \tag{7}$$

The change in $V(d)$ accounts for most of the change in the clathrate inventory due to warming. For example, we can reduce the volume of the clathrate inventory to 15% of the present-day value by decreasing the average depth of the stability zone to d=0.62 d_0. The minimum concentration of organic carbon increases to 2.5% on passive margins and 1.2% on active margins. Such high values of organic carbon greatly reduce the area where clathrate can form.

The effect of warming is clearly illustrated by comparing the vertical distribution of clathrate before and after a temperature increase of 3 °C. Fig. 5 shows the distribution of clathrate at water depths of 1, 1.5, and 2 km prior to warming. The distribution of clathrate at the same depths is shown in Fig. 7 after warming. We see that clathrate has disappeared from a depth of 2 km because the supply of carbon at this depth is no longer sufficient to saturate the pore water with methane (see Fig. 7B). Because the supply of organic material to the sediments is not altered by temperature in our calculation, the disappearance of clathrate at a depth of 2 km is due to increased diffusive losses. At depths of 1 and 1.5 km, the volume fractions of clathrate and gas bubbles after warming are slightly smaller than those prior to warming. However, the decrease in volume fraction has only a modest influence on the inventory. The largest effect is due to the reduction in the range of water depths (and hence seafloor area) where clathrate can form.

5.2. Changes in O_2 concentration

Organic carbon burial in sediment is sensitive to the concentration of oxygen in the overlying water. Lower deep-ocean oxygen concentrations could therefore drive an increase in clathrate abundance by increasing the methane supply rate to the clathrate zone. The minimum concentration of organic matter required to drive clathrate formation (~1% in the present-day ocean) is unchanged by a change in deep oxygen, but the area where such sediments are found increases greatly when oxygen levels are lower. We predict the effect of oxygen levels by computing the apparent oxygen utilization (AOU) of the present-day ocean as the potential disequilibrium of each subsurface water parcel, relative to atmospheric oxygen at the sea surface. Deep ocean oxygen is decreased by linearly increasing the observed, AOU, and vice versa. Even a modest 40-μM decrease in O_2 concentration is sufficient to increase in the methane inventory by a factor of 2 (Fig. 7B). Conversely, a 40-μM

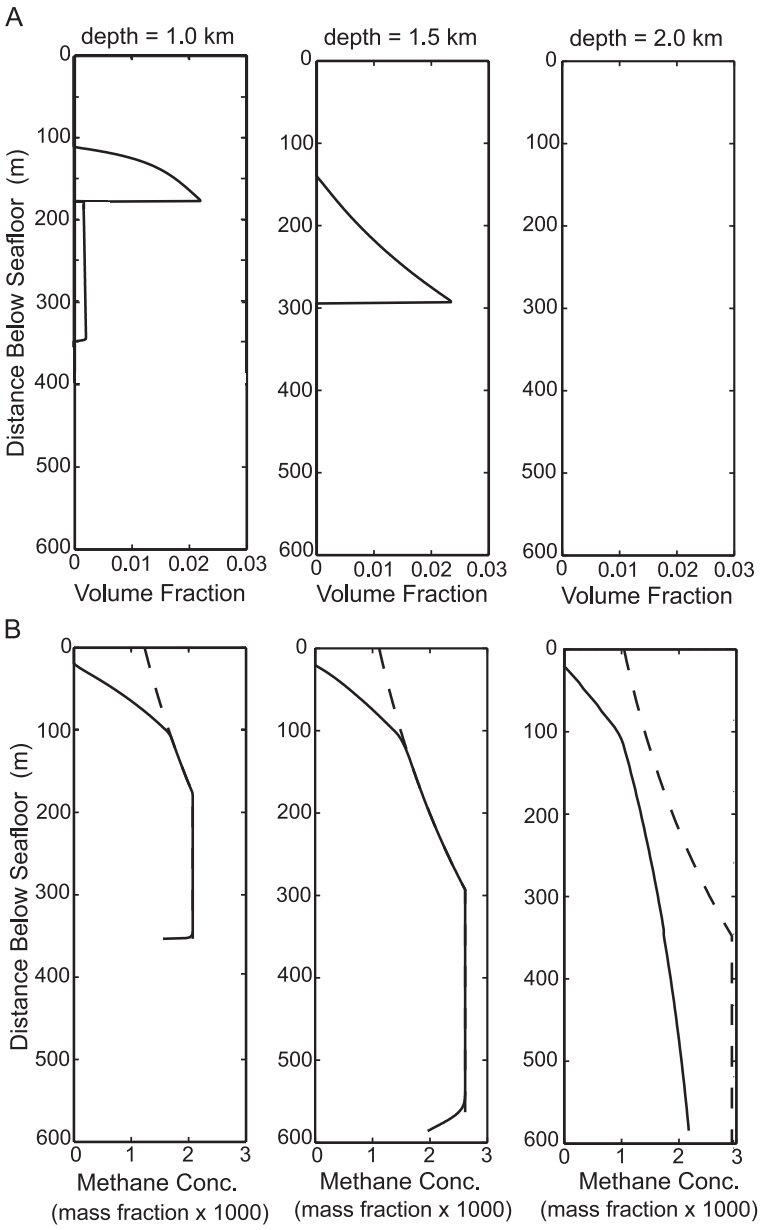

Fig. 7. Vertical distribution of (A) clathrate and bubble volumes and (B) the concentration of dissolved methane below the seafloor under passive-margin conditions. The water depth and O_2 concentration coincide with the values chosen in Fig. 5, but the seafloor temperature is 3 °C warmer. Clathrate does not form at a depth of 2 km because the supply of organic carbon does not permit the concentration of dissolved methane to exceed the local solubility (dashed line in B).

increase in the O_2 concentration lowers the inventory of methane by a factor of 2. More significant increases are possible if regions of the ocean were to become anoxic for ~10^6 years (allowing sufficient time for clathrate accumulation).

The concentration of O_2 may be important for assessing the size of the clathrate inventory in the past when the ocean was warmer. It is thought that the deep-ocean temperature in Paleocene, prior to an abrupt warming event 55 Ma ago, was probably 5 °C

warmer than present. If the ocean at that time was otherwise similar to the ocean today, then our calculations suggest that the steady-state inventory of methane was insufficient to explain the magnitude of the excursion in $\delta^{13}C$ [15]. We can restore clathrate as a viable source of carbon for the isotopic excursion by appealing to a lower O_2 concentration in the ocean. For example, our calculations suggest that several thousand Gton C could be stored in clathrate below an anoxic Arctic Ocean.

5.3. Changes in the rate of carbon rain

Changes in primary production under warmer conditions can alter the clathrate inventory by altering the rate of carbon rain to the seafloor. An increase in carbon rain during the Paleocene has been evoked to explain the occurrence of a large clathrate reservoir when the deep ocean is warm [15]. We alter the rate of carbon rain in the model using one of two assumptions. In one case, we assume that the ratio of organic carbon to clay is fixed. An increase in carbon rain implies an increase in sedimentation rate without substantially altering the concentration of organic carbon. In the second case, we increase the carbon rain without altering the clay rain. The sedimentation rate is effectively unchanged, but the concentration of organic carbon in the sediments increases. We use these two approximations to investigate the effect of a 50% increase in carbon rain. The diagenesis model is rerun with revised inputs, and the results are fed into the clathrate model to determine the global inventory.

The resulting inventory of methane increases by a roughly a factor of 2 in both approximations. Most of the additional methane is stored as bubbles when the sedimentation rate increases, whereas comparable increases in bubble and clathrate volumes occur when the concentration of organic carbon increases. (The bubble volume depends primarily on the flux of clathrate through the base of the stability field. An increase in bubble volume arises from an increase in either the clathrate volume or sedimentation rate). The increase in sedimentation rate also reduces the concentration of organic carbon required to form clathrate. We find that a 50% increase in sedimentation rate reduces the required concentration of organic carbon by almost 50%. However, the change in carbon rain is not sufficient on its own to fully compensate for higher temperature during the Paleocene.

5.4. Changes in sea level

Changes in sea level alter the inventory of clathrate by modifying the pressure at the seafloor. A drop in sea level lowers pressure at the seafloor, causing a reduction in the thickness of the stability zone. The effect on the clathrate inventory is completely analogous to the effect of a temperature change. The main difference is that plausible changes in sea level cause only a small change in the thickness of the stability zone. For example, a 100-m drop in sea level reduces the thickness of the stability zone by less than 10 m in most locations. We predict a 3% decrease in the clathrate inventory when the steady-state model is rerun with a 100-m decrease in sea level. Because sea level has only a small influence on the clathrate inventory, we expect cooler temperatures during glacial periods to produce a net increase in the clathrate inventory.

6. Discussion

Several millions years are required to accumulate a steady inventory [25], whereas the decline due to warming may be comparatively rapid [15]. This asymmetry in the time scale for growth and decline affects the clathrate inventory when conditions vary. For example, glacial periods favor larger inventories because the effect of cool conditions should prevail over the effect of lower sea level. On the other hand, rapid adjustment to warmer interglacial periods may be sufficient to make the present inventory compatible with steady-state predictions based on current (interglacial) conditions. A substantial decrease in the clathrate inventory is expected in the future as temperatures exceed those experienced in the past few million years. Lower O_2 concentrations or higher rates of carbon rain cannot offset the effects of higher temperatures because the clathrate reservoir grows slowly in response to changes.

Several mechanisms have been proposed to permit a rapid release of methane from clathrate. Submarine slides can release regional accumulations of clathrate

and bubbles in a matter of minutes. Failure is thought to occur in response to elevated pressure in the pore water because the phase change from clathrate to methane and water involves a volume increase [20]. The factors that contribute to failure include the abundance of clathrate, the magnitude of warming and the permeability of the sediments. It is not known if future warming is sufficient to cause failure of continental slopes on a global scale, but isotopic evidence of rapid carbon release in the past is suggestive.

A more recent proposal for rapid release of methane is based on elevated pressure in the gas phase [21,44]. Interconnection of gas bubbles below the clathrate stability zone transmits hydrostatic pressures from greater depths by virtue of the low density of the gas phase. The excess (nonhydrostatic) pressure at the top of the gas layer may be sufficient to fracture the sediments and drive gas toward the seafloor. Evidence for gas escaping through the seafloor on the Blake Ridge suggests that this process is possible [47]. However, it is not clear if the process occurs on most continental margins. The volume fraction of gas needed for interconnection is thought to be about 10% [21], which is substantially higher than the typical volume predicted in our calculations. In fact, most clathrate locations are predicted have gas volumes less than 1% of the pore volume, which is at the limit of detection in geophysical surveys [48,49]. Whether larger volumes of gas develop during the transient response to warming remains to be determined using time-dependent models.

7. Conclusions

We use a steady-state model to predict the present-day inventory of methane clathrate below the seafloor. Our best estimate yields 3×10^{18} g C in clathrate and 1.8×10^{18} g C in bubbles. The largest source of uncertainty is due to the efficiency of methane production from organic matter and to the rate of vertical fluid flow. Values for these parameters are taken from previous modeling studies at both passive and active margins.

Changes in the clathrate inventory are predicted using plausible changes in the deep ocean. A warming of 3 °C reduces the clathrate inventory to 15% of its present value. Much of this decrease is attributed an increase in the organic carbon needed to sustain clathrate in sediments when the zone of stability becomes thin. The area of seafloor with sufficient organic carbon drops sharply as the stability zone gets thinner. A reduction in sea level has a similar effect, although the change in the inventory is small because the depth of the stability zone is typically altered by less than 10 m for a nominal 100-m drop in sea level.

Future warming implies substantial changes in the clathrate inventory. However, our calculations do not predict the time scale for this adjustment. Several mechanisms permit rapid release of methane, and it appears that one or more of these mechanisms must have operated at the end of the Paleocene if the excursion in $\delta^{13}C$ is caused by a total collapse of the clathrate inventory. On the other hand, the clathrate reservoir prior to this collapse may have been insufficient to explain the isotopic excursion because the deep ocean was warmer than today. One way to increase the clathrate inventory is to lower the concentration of dissolved O_2. We show that a 40-μM decrease in O_2 concentration can increase the clathrate inventory by a factor of 2. Similarly, a 50% increase in the rate of carbon rain can also increase the clathrate inventory by a factor of 2.

Acknowledgements

We thank Peter Brewer, Jerry Dickens and Mark Maslin for many constructive comments and suggestions.

Appendix A. Supplementary data

Supplementary data associated with this article can be found, in the online version, at doi:10.1016/j.epsl.2004.09.005.

References

[1] D.E. Archer, J.L. Morford, S.R. Emerson, A model of suboxic sedimentary diagenesis suitable for automatic tuning and gridded global domains, Glob. Biogeochem. Cycles 16 (2002) doi:10.1029/2000GB001288.

[2] M.K. Davie, B.A. Buffett, A steady state model for marine hydrate formation: constraints on methane supply from pore water sulfate profiles, J. Geophys. Res. 108 (B10) (2003) doi:10.1029/2002JB002300.
[3] K.A. Kvenvolden, Methane hydrate—a major reservoir of carbon in the shallow geosphere, Chem. Geol. 71 (1–3) (1988) 41–51.
[4] G.J. MacDonald, The future of methane as an energy resource, Annu. Rev. Energy 15 (1990) 53–83.
[5] V. Gornitz, I. Fung, Potential distribution of methane hydrate in the world's oceans, Glob. Biogeochem. Cycles 8 (1994) 335–347.
[6] E.T. Sundquist, Geological perspectives on carbon dioxide and the carbon cycle, in: W.S.B.E.T. Sundquist (Ed.), The Carbon Cycle and Atmospheric CO2: Natural Variations Archean to Present, vol. 32, American Geophysical Union, Washington, DC, 1985, p. 5.
[7] K.A. Kvenvolden, Methane hydrates and global climate, Glob. Biogeochem. Cycles 2 (1988) 221–229.
[8] G.J. MacDonald, Role of methane clathrates in past and future climates, Clim. Change 16 (1990) 247–281.
[9] J.P. Kennett, K.G. Cannariato, I.L. Hendry, R.J. Behl, Carbon isotopic evidence for methane hydrate instability during quaternary interstadials, Science 288 (2000) 128–133.
[10] G.R. Dickens, J.R. O'Neil, D.K. Rea, R.M. Owens, Dissociation of oceanic methane hydrate as a cause of the carbon isotope excursion at the end of the Paleocene, Paleoceanography 10 (1995) 965–971.
[11] J.P. Kennett, L.D. Stott, Abrupt deep sea warming, paleoceanographic changes and benthic extinctions at the end of the Paleocene, Nature 353 (1991) 225–229.
[12] E. Thomas, N.J. Shackleton, The Paleocene–Eocene benthic foraminiferal extinction and stable isotope anomalies, Spec. Publ.-Geol. Soc. Lond. 101 (1996) 401–411.
[13] P.L. Koch, J.C. Zachos, P.D. Gingerich, Coupled isotopic change in marine and continental carbon reservoirs near the Paleocene/Eocene boundary, Nature 358 (1992) 319–322.
[14] M.E. Katz, D.K. Pak, G.R. Dickens, K.G. Miller, The source and fate of massive carbon input during the latest Paleocene thermal maximum, Science 286 (1999) 1531–1533.
[15] G.R. Dickens, Rethinking the global carbon cycle with a large, dynamic and microbially mediated gas hydrate capacitor, Earth Planet. Sci. Lett. 213 (2003) 169–183.
[16] G.R. Dickens, Methane oxidation during the late Paleocene thermal maximum, Bull. Soc. Geol. Fr. 171 (2000) 37–49.
[17] D. Archer, H. Kheshgi, E. Maier-Riemer, Multiple timescales for neutralization of fossil fuel CO_2, Geophys. Res. Lett. 24 (1997) 405–408.
[18] G.R. Dickens, The potential volume of oceanic methane hydrates with variable external conditions, Org. Geochem. 32 (2001) 1179–1193.
[19] W.S. Borowski, C.K. Paull, W. Ussler, Carbon cycling within the methanogenic zone of continental rise sediments: an example from methane-rich sediments overlying the Blake Ridge gas hydrate deposits, Mar. Chem. 57 (1997) 299–311.
[20] R.E. Kayen, H.J. Lee, Pleistocene slope instability of gas hydrate-laden sediment of Beaufort Sea margin, Mar. Geotechnol. 10 (1991) 125–141.
[21] B.P. Flemings, X. Liu, W.J. Winters, Critical pressure and multiphase flow in Blake Ridge gas hydrates, Geology 31 (2003) 1057–1060.
[22] L.D.D. Harvey, Z. Huang, Evaluation of the potential impact of methane clathrate destabilization on future global warming, J. Geophys. Res. 100 (1995) 2905–2926.
[23] A.V. Milkov, G.E. Claypool, Y.-J. Lee, W. Xu, G.R. Dickens, W.S. Borowski, O.L.S. Party, In situ methane concentrations at Hydrate Ridge, offshore Oregon: new constraints on the global gas hydrate inventory from an active margin, Geology 31 (2003) 833–836.
[24] A.V. Milkov, Global estimates of hydrate-bound gas in marine sediments: how much is really out there? Earth Sci. Rev. 66 (2004) 183–197.
[25] M.K. Davie, B.A. Buffett, A numerical model for the formation of gas hydrate below the seafloor, J. Geophys. Res. 106 (B1) (2001) 497–514.
[26] K.A. Kvenvolden, Gas hydrates—geological perspective and global change, Rev. Geophys. 31 (2) (1993) 173–187.
[27] G.E. Claypool, K.A. Kvenvolden, Methane and other hydrocarbon gases in marine sediment, Annu. Rev. Earth Planet. Sci. 11 (1983) 299–327.
[28] W.S. Holbrook, H. Hoskins, W.T. Wood, R.A. Stephen, D. Lizzaralde, Methane hydrate and free gas on the Blake Ridge from vertical seismic profiling, Science 273 (1996) 1840–1843.
[29] T. Yuan, R.D. Hyndman, G.D. Spence, B. Desmons, Seismic velocity increase and deep-sea gas hydrate concentration above a bottom-simulating reflector on the northern Cascadia continental slope, J. Geophysical Res., B 101 (1996) 13655–13671.
[30] R.D. Hyndman, T. Yuan, K. Moran, The concentration of deep sea gas hydrates from downhole electrical resistivity logs and laboratory data, Earth Planet. Sci. Lett. 172 (1999) 167–177.
[31] R.D. Hyndman, E.E. Davis, A mechanism for the formation of methane hydrate and seafloor bottom simulating reflectors by vertical expulsion, J. Geophys. Res. 97 (1992) 7025–7041.
[32] R.D. Hyndman, G.F. Moore, K. Moran, Velocity, porosity, and pore-fluid loss from the Nankai subduction zone accretionary prism, Proc. Ocean Drill. Program Sci. Results 131 (1993) 211–220.
[33] M.K. Davie, B.A. Buffett, Sources of methane for marine gas hydrate: inferences from a comparison of observations and numerical models, Earth Planet. Sci. Lett. 206 (1–2) (2003) 51–63.
[34] D.E. Archer, A data-driven model of the global calcite lysocline, Glob. Biogeochem. Cycles 10 (1996) 511–526.
[35] D. Burdige, J.M. Geiskes, A pore water/solid phase diagenetic model for manganese in marine sediments, Am. J. Sci. 283 (1983) 29–47.
[36] P.v. Cappellen, Y. Wang, Cycling of iron and manganese in surface sediments: a general theory for the coupled transport

and reaction of carbon, oxygen, nitrogen, sulfur, iron and manganese, Am. J. Sci. 296 (1996) 197–243.
[37] K.A. Kvenvolden, A review of the geochemistry of methane in natural gas hydrate, Org. Geochem. 23 (1995) 992–1008.
[38] M.K. Davie, O.Y. Zatsepina, B.A. Buffett, Methane solubility in marine hydrate environments, Mar. Geol. 203 (2004) 177–184.
[39] I. Hutchinson, The effect of sedimentation and compaction on oceanic heat flow, Geophys. J. R. Astron. Soc. 82 (1985) 439–459.
[40] B. Dugan, P.B. Flemings, Overpressure and fluid flow in the New Jersey continental slope: implications for slope failure and cold seeps, Science 289 (2000) 288–291.
[41] S. Levitus, M.E. Conkright, J.L. Reid, R.G. Najjar, A. Mantyla, Distribution of nitrate, phosphate, and silicate in the world's oceans, Prog. Oceanogr. 31 (1993) 245–273.
[42] G.K. Westbrook, B. Carson, R.J. Musgrave, et al., Proceedings of the Ocean Drilling Program, in: Initial Reports, vol. 146, 1994, College Station, TX.
[43] C.K. Paull, R. Matsumoto, P.J. Wallace, et al., Proceeding of the Ocean Drilling Program, in: Initial Reports, vol. 164, 1996, College Station, TX.
[44] M.J. Hornbach, D.M. Saffer, W.S. Holbrook, Critically pressured free-gas reservoirs below gas hydrate provinces, Nature 427 (2004) 142–144.
[45] R.J. Stouffer, S. Manabe, Response of a coupled ocean-atmosphere model to increasing atmospheric carbon dioxide: sensitivity to the rate of increase, J. Climate 12 (8) (1999) 2224–2237.
[46] S. Manabe, R.J. Stouffer, Multiple-century response of a coupled ocean-atmosphere model to an increase of atmospheric carbon dioxide, J. Climate 7 (1994) 5–23.
[47] A.R. Gorman, W.S. Holbrook, M.J. Hornbach, K.L. Hackwith, D. Lizarralde, I. Pecher, Migration of methane gas through a hydrate stability zone in a low-flux hydrate province, Geology 30 (2002) 327–330.
[48] W. Wood, P. Stoffa, T. Shipley, Quantitative detection of methane hydrate through high-resolution seismic velocity analysis, J. Geophys. Res. 99 (1994) 9681–9695.
[49] I.A. Pecher, T.A. Minshull, S.C. Singh, R.v. Huene, Velocity structure of a bottom simulating reflector offshore Peru: results from full waveform inversion, Earth Planet. Sci. Lett. 139 (1996) 459–469.
[50] E.D. Sloan, Clathrate Hydrates of Natural Gas, Marcel Dekker, New York, 1998.